Manuscript submitted to Journal of Cleaner Production

Idle Vehicle Relocation Strategy through Deep Learning for Shared Autonomous Electric Vehicle System Optimization

Seongsin Kim[1]
Department of Mechanical Systems Engineering, Sookmyung Women's University,
Seoul 04310, South Korea
kss@sm.ac.kr

Ungki Lee[1]
Department of Mechanical Engineering, Korea Advanced Institute of Science and Technology,
Daejeon, 34141, South Korea
lwk920518@kaist.ac.kr

Ikjin Lee[*]
Department of Mechanical Engineering, Korea Advanced Institute of Science and Technology,
Daejeon, 34141, South Korea
ikjin.lee@kaist.ac.kr

Namwoo Kang[*]
The Cho Chun Shik Graduate School of Green Transportation,
Korea Advanced Institute of Science and Technology, 34141 Daejeon, Korea
nwkang@kaist.ac.kr

[1]Contributed equally to this work.

[*]Corresponding authors

Abstract

In optimization of a shared autonomous electric vehicle (SAEV) system, idle vehicle relocation strategies are important to reduce operation costs and customers' wait time. However, for an on-demand service, continuous optimization for idle vehicle relocation is computationally expensive, and thus, not effective. This study proposes a deep learning-based algorithm that can instantly predict the optimal solution to idle vehicle relocation problems under various traffic conditions. The proposed relocation process comprises three steps. First, a deep learning-based passenger demand prediction model using taxi big data is built. Second, idle vehicle relocation problems are solved based on predicted demands, and optimal solution data are collected. Finally, a deep learning model using the optimal solution data is built to estimate the optimal strategy without solving relocation. In addition, the proposed idle vehicle relocation model is validated by applying it to optimize the SAEV system. We present an optimal service system including the design of SAEV vehicles and charging stations. Further, we demonstrate that the proposed strategy can drastically reduce operation costs and wait times for on-demand services.

Keywords: Idle vehicle relocation, deep learning, shared autonomous electric vehicle (SAEV), demand prediction, system optimization

1. Introduction

Shared autonomous electric vehicles (SAEVs) that combine car sharing services, autonomous driving technology, and electric vehicles (EVs) are expected to revolutionize transportation systems in the near future [1,2]. An SAEV autonomously goes to the location requested by a customer and rides that customer to a prescribed destination, thus providing a low-stress and safe transportation service [3,4], promoting transportation accessibility [5], and reducing mobility costs [6]. In addition, EVs help reduce fuel consumption and produce less environmental pollutants and greenhouse gas emissions [7–10]. Consequently, several studies related to operation and optimization of SAEV systems were conducted on the basis of SAEV simulations [1,11–15].

SAEV system optimization determines the optimal vehicle size and specifications, as well as the number and location of charging stations (CSs) based on the SAEV operation. A primary issue regarding SAEV operation is the behavior or movement of idle vehicles. Most SAEV studies selected randomly moving strategies or implemented free-floating systems where the vehicles park at the current location or at a designated parking spot [15–19]. However, during practical SAEV operation, parking in the middle of the road is unrealistic. It is more efficient to move in advance to a location where passenger demands are expected than to move the vehicle around randomly. Further, customers' wait time can be reduced by predicting the passenger demands and preemptively moving idle vehicles to an appropriate destination, resulting in reduction of the required fleet size, the number of CSs, and costs [20–27]. Previous research related to this study is reviewed in Section 2.

Previous studies proposed an idle vehicle relocation strategy based on optimization, but research with the use of deep learning was lacking. To embody on-demand service, implementing real-time decision-making based on big data is necessary. Therefore, deep learning is required to approximate a complex optimization process and reduce the computational cost. Several previous studies predicted passenger demand using deep learning. However, studies on the use of predictive models for SAEV system optimization are few.

This study proposes a deep learning-based idle vehicle relocation strategy and presents an SAEV vehicle and CS design framework that can minimize SAEV operation costs using the proposed strategy. The proposed idle vehicle relocation strategy is based on passenger demand prediction, which is obtained using deep learning. This strategy was not considered in previous studies. It enables optimal idle vehicle relocation according to the predicted passenger demand. Furthermore, the approximation of the optimization process using deep learning makes performing idle relocation in real-time possible. The proposed idle vehicle relocation strategy reduces customer wait time by improving the efficiency of fleet operation. Therefore, by performing SAEV system optimization using the proposed idle vehicle relocation strategy based on deep learning instead of the strategy based on optimization used in previous studies, SAEV operation costs can be lowered further, thereby lowering the burden on customers and companies that operate SAEV, which in turn helps the generalization and popularization of SAEV. The effectiveness of the proposed framework is verified by utilizing big data for taxi services in Seoul. The rest of this manuscript is structured as follows. In Section 3, the proposed framework is introduced. In Section 4, each step of the proposed framework is described in detail. The SAEV system optimization problems and models are discussed in Section 5. In Section 6, the simulation results are presented and discussed. Finally, Section 7 concludes the study and provides directions for future work.

2. Related Works

2.1. SAEV System Optimization

Several studies to optimize the SAEV fleet operation based on simulation were conducted. Chen et al. simulated the performance characteristics of SAEVs that provide service to travelers all over Austin, Texas [11]. They studied the extent to which the response time can be improved when the charging time is reduced or when the number of vehicles is increased. Idle vehicle relocation was performed in consideration of expected demand. However, the demand prediction model was not used, and the simple balance of the number of vehicles was the only focus. Kang et al. presented an SAEV system optimization framework integrating vehicle design, charging station locations, and fleet size and assignment [12]. This study compared the optimization results of an SAEV with those of a shared autonomous vehicle using internal combustion engine. However, free-floating system is applied to idle vehicle relocation, which is a limitation. Farhan et al. proposed an SAEV simulation framework that integrated optimization and discrete events and solved the routing optimization problem [13]. This study also used the idle vehicle relocation strategy to simply balance the number of vehicles without using the demand

prediction model. Zhao et al. proposed a station-based SAEV system model for the simultaneous optimization of CS relocation and fleet size [14]. In this study, the idle vehicle stayed in a parking lot, and the vehicles were moved to maintain the number of vehicles initially allocated to the parking lot. Loeb et al. applied a sizing strategy for a specific vehicle based on response time, empty vehicle-miles-travelled, and replacement rate [19]. They demonstrated that long-range and high-speed charging EVs are better than short-range and slow-charging vehicles. However, idle vehicle movements are not modeled in the simulation. Lee et al. considered the uncertainties in SAEV systems and introduced reliability-based design optimization to derive an optimal SAEV system design that minimizes the total cost while satisfying the target reliability of the customer's wait time [15]. A limitation of this study is that the random-motion strategy is used for idle vehicle relocation. Melendez et al. proposed a cyber-physical system (CPS) comprising a large fleet of SAEVs and a set of charging hubs for optimal planning and real-time operations [28]. In this study, the idle state vehicles are set to pay a parking fee and stay in the parking lot. In the above studies, a significant change in SAEV system optimization results is expected if idle vehicle relocation strategy is implemented, considering that the demand predication model is used. Yi and Smart proposed a decision-making framework that integrates dispatching and charging management based on a system optimization approach [29]. The proposed framework aims to reduce operational costs while increasing fleet revenue.

2.2. Idle Vehicle Relocation Strategy

Several studies were conducted on the positioning of idle vehicles, which have a considerable influence on the future demand and operation of SAEVs. Phithakkitnukoon et al. studied error-based learning through an inference engine based on a naïve Bayesian classifier and developed a prediction model for the number of empty taxis according to time and weather conditions [20]. Such a model exhibits a limitation as it does not reflect the real world well because it applies small-fleet samples. Yuan et al. proposed a parking-spot detection-based probability model algorithm that recommends passengers to access empty taxis using information about a high-income taxi driver's pickup action [21]. However, this model has the limitation that it does not integrate real-time traffic information. Li et al. transformed the digital tracking of Hangzhou 5350 taxis into a taxi pattern table and training/testing data set [22]; thus, they developed a taxi pattern determination algorithm for efficient passenger search through data mining algorithms. Zhang et al. proposed a dynamic bike relocation methodology to transform the model into an equivalent mixed-integer problem model and a heuristic algorithm to solve the dynamic bicycle repositioning problem (BRP) [3]. A demand forecasting model that assumes that pick-up and drop-off patterns follow a non-homogeneous Poisson process was used. Sayarshad and Chow proposed a queueing-based formula to solve the idle vehicle relocation problem [24]. A Lagrange-decomposition heuristic algorithm that estimates the arrival process parameters for simulation using data from 5 days a week for six nodes was proposed and compared with a relaxed lower bound solution. Wen et al. used a model-free reinforcement learning approach that adopted a deep Q network for idle vehicles to resolve the imbalance between vehicle supply and passenger demand [25]. It was applied to an agent-based simulator and tested in a case study conducted in London. However, the study was limited with the fact that it assumes that the predicted demand follows the Poisson process instead of using the demand prediction model. Ma et al. proposed a ridesharing strategy using queueing theoretical vehicle dispatch and an idle vehicle relocation algorithm with integrated transit that picks up the passengers at home or at a transit station [26]. Pouls et al. proposed a prediction-based relocation algorithm using a mixed-integer programming model for idle vehicle relocation [27]. Real-time data sets from Hamburg, New York City (NYC) and Manhattan were used to demonstrate the suitability of this algorithm for real-time use. However, the algorithm proposed in this study did not reflect the characteristics of vehicles that continuously move on the road in real practice. de Souza et al. proposed an optimization-based repositioning strategy for shared autonomous vehicle that moves excess fleets to another area with insufficient fleet supply [30]. The repositioning strategy results in an increase in the share of served requests and a decrease in customer wait time. Dean et al. proposed an optimization framework that couples the charging and repositioning of SAEV [31]. They applied the framework to the Austin,Texas regions and the results showed that customer wait time and empty travel decreased, and average daily trips served per SAEV increased. However, the proposed framework has a limitation that it does not use a model that provides predicted demand in real time. In summary, the abovementioned studies indicate the need for a strategy that considers the predicted demand provided by the demand prediction model, created based on the demand data, and that performed the optimal idle vehicle relocation suitable for real practice in real-time.

2.3. Passenger Demand Prediction by Deep Learning

Deep learning-based studies that predict passenger demand for shared vehicles such as taxis achieved good performance. DeepST extracted spatiotemporal features by preprocessing the taxi demand data into an image

formed as a grid array and inputting such image in a convolution layer [23]. The prediction performance was improved by using external information such as weather data; however, identifying similar patterns that repeat at specific cycles is difficult. DMVST-Net extracted the spatiotemporal and semantic contexts by converting 20×20 images into small 7×7 images and applying a local convolutional neural network (CNN), long short-term memory (LSTM), and graph embedding that use taxi demand data in Guangzhou City [32]. They extracted the semantic context through large-scale information network embedding (LINE), which is a graph embedding method. STDN used data in a particular time slot together with different data extracted in the past, beyond the past 4 hours of NYC's taxi data [33]. However, as the time range of input data widened, the gradient vanishing phenomenon intensified and training became difficult. The problem was solved by training the slot that has to concentrate with the periodically shifted attention mechanism, which is a temporal attention method. The TGNet model used the pickup and drop-off data of NYC taxi and the hidden pattern of time data to carry out training using only temporal guided embedding [34]. Thus, representing time, day of the week, holiday or not, and the day before holiday or not, they could train complex spatiotemporal patterns with a simple architecture. Xu et al. predicted the station demand and shared bicycle demand in real time using an LSTM neural network [35]. They predicted the shared bicycle demand in Nanjing, China, and the passenger demand and mobility patterns of bicycle sharing without station. Chen et al. extracted the spatial-pattern distribution using a graph convolutional network (GCN), and the temporal feature of the traffic flow using LSTM; they performed predictions about road sections [36]. Several studies on passenger demand prediction by deep learning have been reported. However, studies on SAEV system optimization using these predictive models are limited. Therefore, an opportunity to improve the SAEV system optimization results can emerge through the development of an idle vehicle relocation strategy based on these predictive models.

3. Proposed Framework

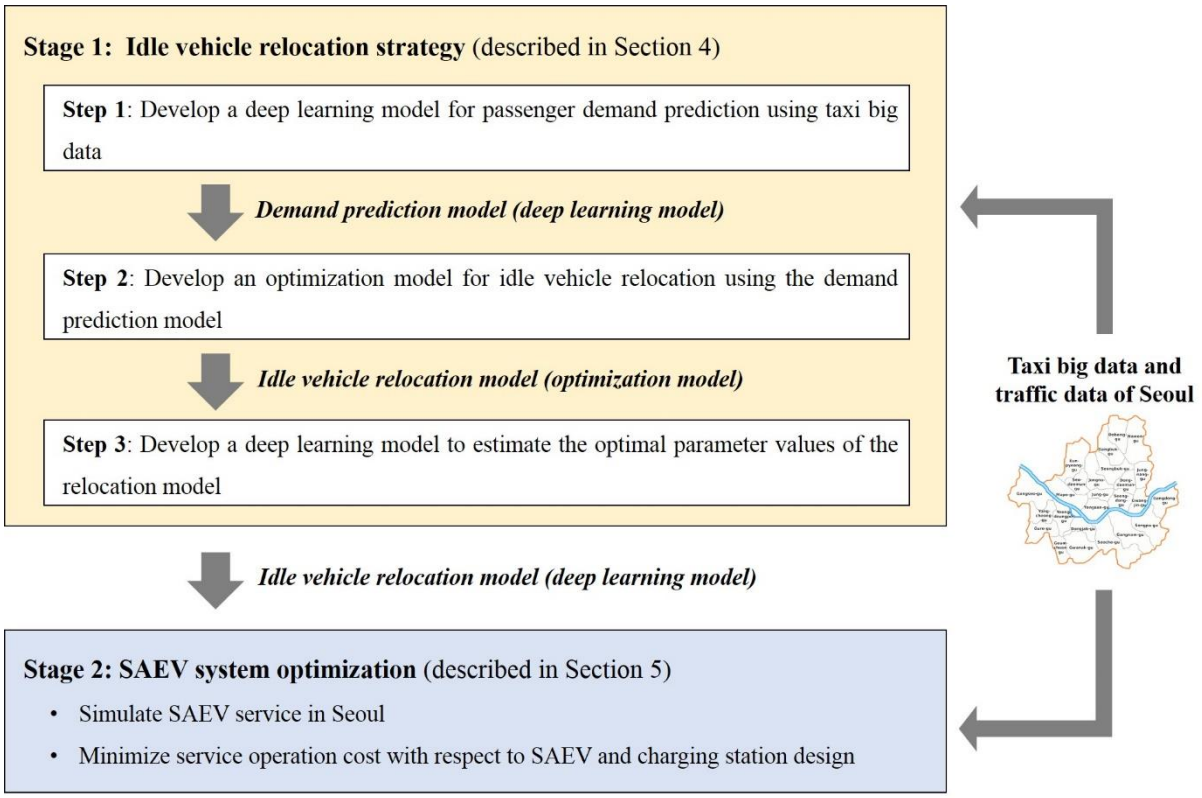

Fig. 1. Deep learning-based idle vehicle relocation strategy and SAEV system optimization.

The proposed framework entails two stages, as shown in Fig. 1. The data used for model development were the Seoul City's taxi-call big data provided by the Seoul Metropolitan Government (SEO-Taxi), collected over 15

months—from August, 2015, to October, 2016 [37].

Stage 1 proposes a deep learning-based idle vehicle relocation strategy. The deep learning model that trained the idle vehicle relocation solution was optimized for various traffic conditions in the past with end-to-end learning. Thus, it can decide the destination where the idle vehicle has to be placed according to given traffic conditions in the future. The proposed strategy takes place through Step 3 of the sequential model development.

Step 1 builds up a graph neural network (GNN)-based deep learning model that can predict the location and frequency of the passenger demand that will be known 30 minutes later based on the passenger demand location and frequency data; these data include information obtained from the previous 4 hours. In this study, we used the TGNet architecture and improved the performance by adding weather data as supplementary data [34].

Step 2 proposes an optimization model that decides the idle vehicle relocation based on passenger demand predicted through the demand prediction developed in Step 1. The model input comprises location and frequency of passenger demands, status of vehicles, and CS congestion, and the output is expressed in terms of the probability distribution of the idle vehicle destination.

Step 3 proposes a deep learning model that can decide the parameter values of the relocation model developed in Step 2 without going through optimization. Finding a solution by optimization based on various changing traffic conditions from big data is not suitable for on-demand service. Therefore, an approximation model that can propose an immediate solution as an alternative to the optimization model, which has high computational cost, is required. This step produces parameters P_2 and P_3, which are optimized according to the past traffic data used in Step 1, builds a data set, and conducts training with deep learning. The input data are transformed into 2D to represent the location information and are used for training a CNN-based model, which immediately calculates the values of P_2 and P_3.

In Stage 2, the proposed idle vehicle relocation strategy is applied to the SAEV system optimization problem. As a result, a service system design is proposed that can reduce the SAEV operation cost while satisfying the customer's wait time constraint. Using the deep learning prediction model and the idle vehicle relocation model developed in the previous stage, we simulated Seoul City's SAEV operation and determined the SAEV fleet size, battery design, location and number of CSs, and number of chargers in each station that can reduce the operation cost.

4. Idle Vehicle Relocation Strategy

4.1. Step 1: Passenger Demand Prediction by Deep Learning

The data used in the model for passenger demand prediction are the Seoul City's taxi call big data (08/01/2015~10/31/2016, 458 days). These data went through preprocessing, as shown in Fig. 2. We transformed the Seoul City's public taxi data set into a grid cell expression using the number of features in each grid (e.g., interest points and road segments) and the total length of the input features (e.g., road segments). To simplify the location information of passenger demand, we divided Seoul City's area into 2500 grids of 50×50; the area of each grid's cell was approximately 700×700 m^2. To increase the predictability of a smaller area, the map size was set to 50×50. To determine the correlation between the map size and performance, we conducted experiments in which the map recorded low performance when the size of the map was less than 50×50. For instance, in the case of a 20×20 size, the learning time took less than 2 h and was reduced by approximately half of the previous time (4 h). However, the performance results were RMSE 7.59 and MAPE 30.9%. The RMSE was lower by 48.6% compared with the performance in the previous experiment, and the MAPE was improved by 6%. Dividing the map size into more pieces i.e., 100×100 instead of 50×50, slows down learning to a large extent, and the memory efficiency is very low. We finally chose 50×50 as in our base model TGNet, because it efficiently predicted more local regions than 400 (20×20) regions, even if the performance was slightly lower than the case of a 20×20 region for MAPE. We mapped the passenger demand that took place in the corresponding grid cell by counting the requests. The value increases with the demand in the corresponding grid cell, exhibiting a brighter color as the value of the grid cell increases. Each cell represents the taxi-call GPS location and frequency within 30-min units. Each cell's passenger demand within such 30-min periods was added according to the cell locations. To predict the passenger demand that will be known 30 minutes later in the current standard based on a 4-h data period, the images corresponding to 30 minutes were transformed into a 2D image of 8 channels in total (4 h/30 min = 8). The resulting 8 overlapping images became the input data, whereas the 2D 50×50 image of one channel became the output data. Weather data were similarly transformed into 8-channel 2D 50×50 images. The data of the first

12 months were used for training, whereas the remaining 3 months became the test data.

Pickup_ datetime	Dropoff_ datetime	Taxi-call	Pickup_ longitude	Pickup_ latitude
2016-10-01 0:00	2016-10-01 0:18	8	127.0232	37.6031
2016-10-01 0:00	2016-10-01 0:38	3	127.0300	37.5862
2016-10-01 0:00	2016-10-01 0:23	24	127.0300	37.5862
	:		:	

(a)

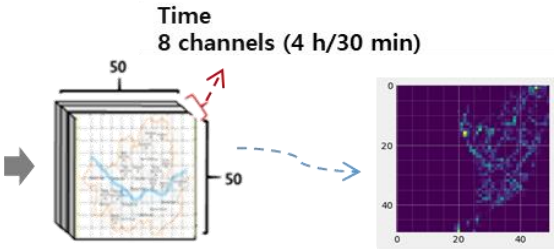

(b) (c)

(a) Preprocessed public data set of Seoul city. Time and the road location where the taxi call occurred, the frequency of taxi calls and the passenger drop-off location.

(b) Map of Seoul is modeled by 700×700 m^2 grids. Frequency of taxi calls every 30 minutes is displayed as a grid, 50×50, combined channels.

(c) An example that showed the passenger demand in the grid cell into an image.

Fig. 2. Data preprocessing steps with Seoul taxi-call data.

For passenger demand prediction, we used TGNet, a deep learning model for prediction of taxi demand [34]. Additionally, trained the weather information of Seoul city by embedding. The deep learning architecture for training is shown in Fig. 3. In this study, the learning rate was set to 0.01, the decay rate was set to 0.01, the batch size was set to 128, the Adam optimizer was used as the optimizer, and early stopping was used to avoid overfitting. The training took approximately 8 h with four GPUs (GTX 1080) operating in parallel.

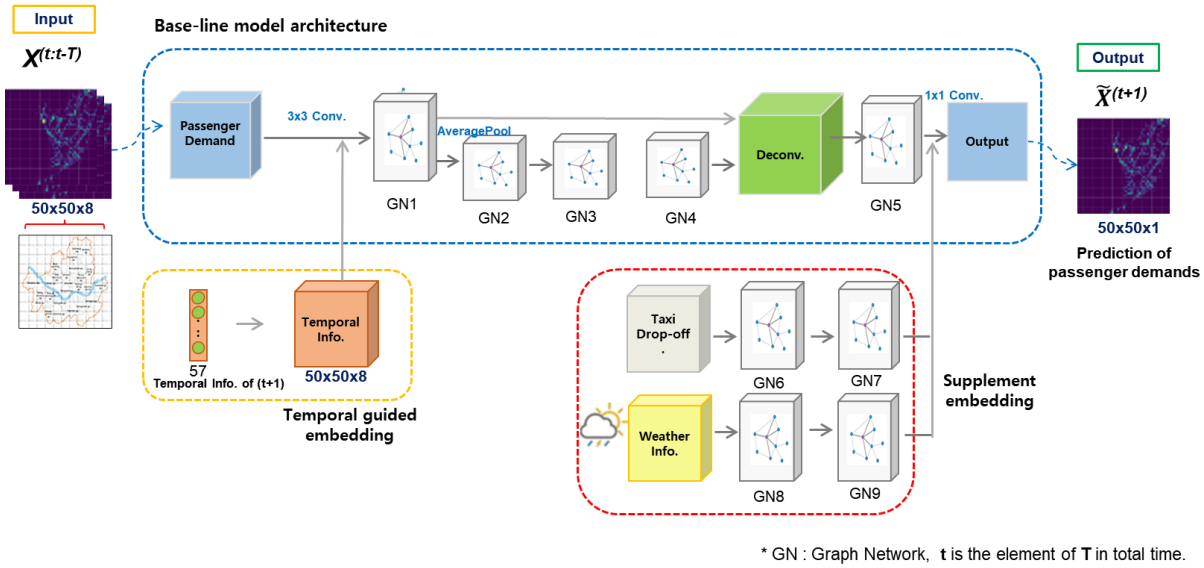

Fig. 3. TGNet model architecture (Base-line + **External Data**).

We used the following temporal information as categorical variables: every 30 min (48); day of the week (7); holiday (1); and the day before a holiday (1). The model in Section 4.1 learns the pattern of taxi demand condition depending on temporal embedding, and the fully convolutional network extracts hidden features of complex space and time. If the model can predict demand by inferring spatio-temporal features according to a condition called a temporal context, then it will learn a similar pattern that is repeated every specific period and temporal information, such as time, day of the week, and whether or not a holiday is celebrated. There was an embedding layer that expresses whether the previous day is a holiday as a continuous real value. The embedding results acted as conditions in the input part of the base model and are used as guides to extract features that are more appropriate to fit the correct answer.

Moreover, TGNet [34] used UNet-structured pooling [38] and skip-connection to learn regional correlations. Average pooling was used to represent the value representing the relationship between the large areas corresponding to the receptive field. In the 1×1 convolution layer, the temporal and spatial correlations were considered simultaneously, and the demand of each region was predicted. In addition, we proposed a structure that can easily utilize external data to increase performance. Each result was concatenated by separately implementing a part that extracted features from past taxi demand data patterns and a part that extracted features from external data. This technique allowed us to incorporate any number of external data into our predictions without modifying the base-line model.

4.2. Step 2: Idle Vehicle Relocation by Optimization

The proposed idle vehicle relocation algorithm starts with selecting the destination of idle-state SAEVs by predicting passenger demands rather than applying random-motion strategies or free floating. The proposed algorithm is based on the passenger demand prediction model presented in Section 4.1. The flowchart of the algorithm is shown in Fig. 4. The passenger demand prediction model provides locations where the passenger demand is predicted to occur and the probability of occurrence (P_1). Thus, the candidates for potential destination can be specified. In addition to P_1, the algorithm considers the probability of selection according to the distance (P_2) and vehicle excess (P_3). P_1, P_2, and P_3 are determined by the predicted frequency of passenger demands, distance from the current location of the vehicle to the candidate, and number of vehicles already assigned that exceeds the predicted passenger demand, respectively. Then, $P_1 \times P_2 \times P_3$ is calculated for all candidates, and the candidate with the highest value is selected as the destination.

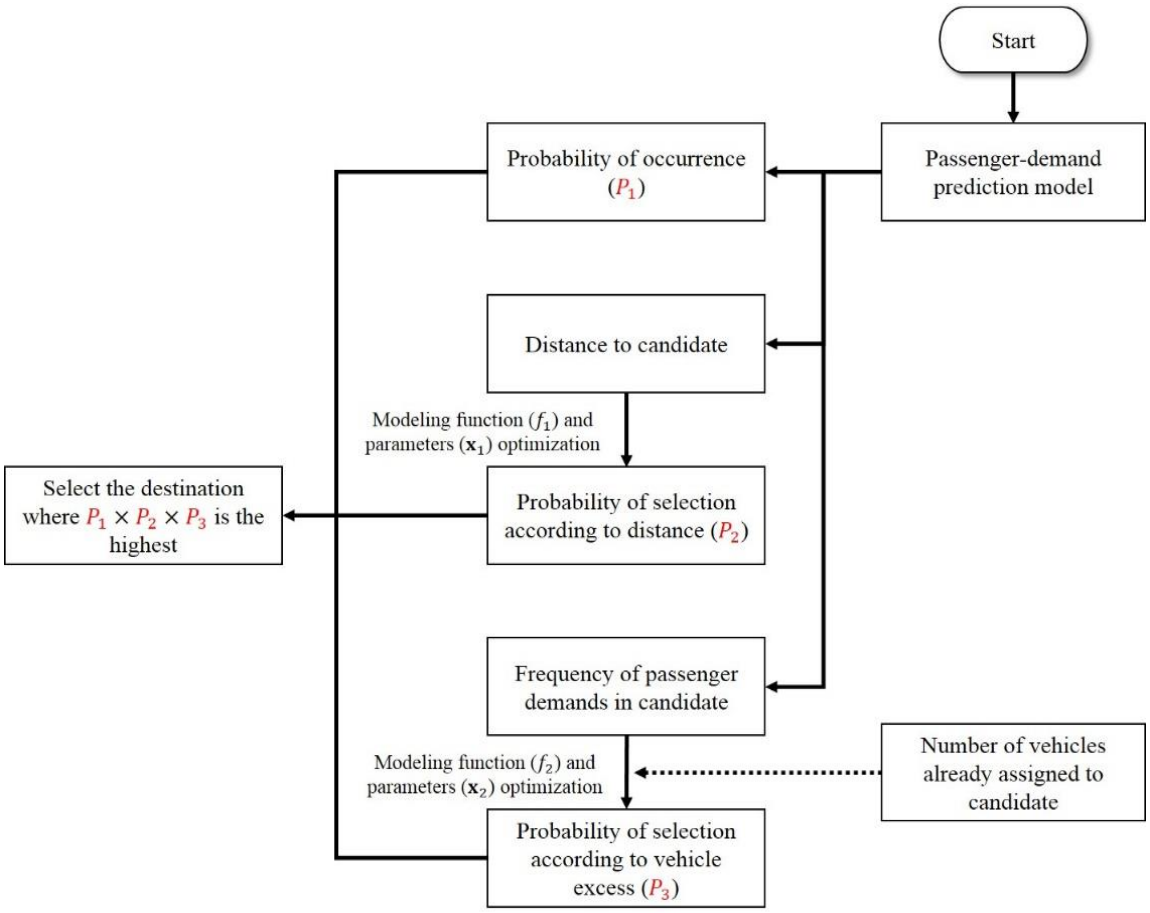

Fig. 4. Flowchart of the destination selection algorithm.

Modeling functions f_1 and f_2 are defined to control the probability of selection according to P_2 and P_3. Modeling functions work such that the candidate with closer distance and less vehicle excess has a high probability of selection. Distance and vehicle excess serve as variables of f_1 and f_2, respectively. Linear, concave, and exponential-Gauss functions summarized in Table 1 are used as candidates for modeling functions. These

functions are commonly used for radial basis functions whose values depend only on the distance between the input and a specific point. These three functions have different characteristics. The characteristics of the functions vary depending on the parameters of each function, e.g., $\mathbf{x}_1$ is the vector of parameters for f_1 and $\mathbf{x}_2$ is the vector of parameters for f_2. The linear function has one parameter, whereas the concave and exponential-Gauss functions have two parameters. Within a given range of variables, the modeling functions take values between 0 and 1. Parameter bounds are set to express the diversity of a given modeling function sufficiently. For each modeling function, the variable O_{ij} represents the distance from the current location i to the destination j for f_1, and the vehicle excess at the destination j for f_2. The value of f_2 is 1, if no vehicle excess occurs. The characteristics of three modeling functions are visualized in Fig. 5 through some examples of functions. Each function shows a different aspect of the slope change with respect to O_{ij} and can be modeled for the entire range of O_{ij} according to the parameter setting. After the modeling functions are selected, parameters are optimized to minimize the mean customer wait time. Overall, the optimization problem can be formulated as follows:

$$\underset{\mathbf{x}_1,\mathbf{x}_2}{\operatorname{argmin}} W\left(\mathbf{x}_1,\mathbf{x}_2\right) \tag{1}$$

where W is the mean customer wait time obtained from SAEV simulation using the passenger demand prediction model and the destination selection algorithm.

Table 1. Modeling function types.

Name	Function	Parameter bounds
Linear	$\max\left\{0, 1-x_1\left\|O_{ij}\right\|\right\}$	x_1: [0,15]
Concave	$\max\left\{0, -x_1\left\|O_{ij}\right\|^{x_2}+1\right\}$	x_1: [0,10], x_2: [1,10]
Exponential-Gauss	$e^{-x_1\left\|O_{ij}\right\|^{x_2}}$	x_1: [0,5], x_2: [0,5]

O_{ij} = Distance from i to j for f_1

$= S_d^j - S_p^j$ for f_2

(S_d^j = number of assigned SAEV, S_p^j = predicted frequency of passenger demands)

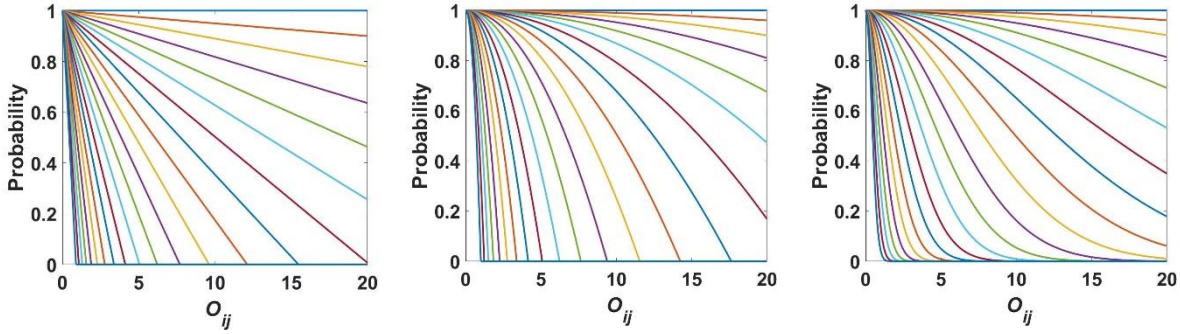

(a) Linear (b) Concave (c) Exponential-Gauss

Fig. 5. Visualization of the three modeling functions.

4.3. Step 3: Idle Vehicle Relocation by Deep Learning

As mentioned in Section 4.2, the optimal modeling functions and parameters of the destination selection algorithm can be obtained through optimization. However, changes in the conditions of an SAEV system, such as location and frequency of passenger demands, congestion of CSs, and status of vehicles, lead to changes in the optimal modeling functions and parameters. Therefore, this section presents a deep learning model that can operate under changing conditions of a given SAEV system by providing optimal modeling functions and parameters for

given conditions in real time. As will be presented in Section 6.1.2, the exponential-Gauss function, which exhibits the best performance, is considered as the optimal modeling function type. Thus, only optimal modeling parameters of the exponential-Gauss function are of interest for deep learning models. The proposed deep learning process is shown in Fig. 6. After obtaining the optimal modeling parameters for given conditions of an SAEV system, the prediction model for modeling parameters can train the relationship between such conditions and optimal modeling parameters. In other words, the prediction model for modeling parameters can provide optimal modeling parameters when the conditions of an SAEV system at a certain moment are given.

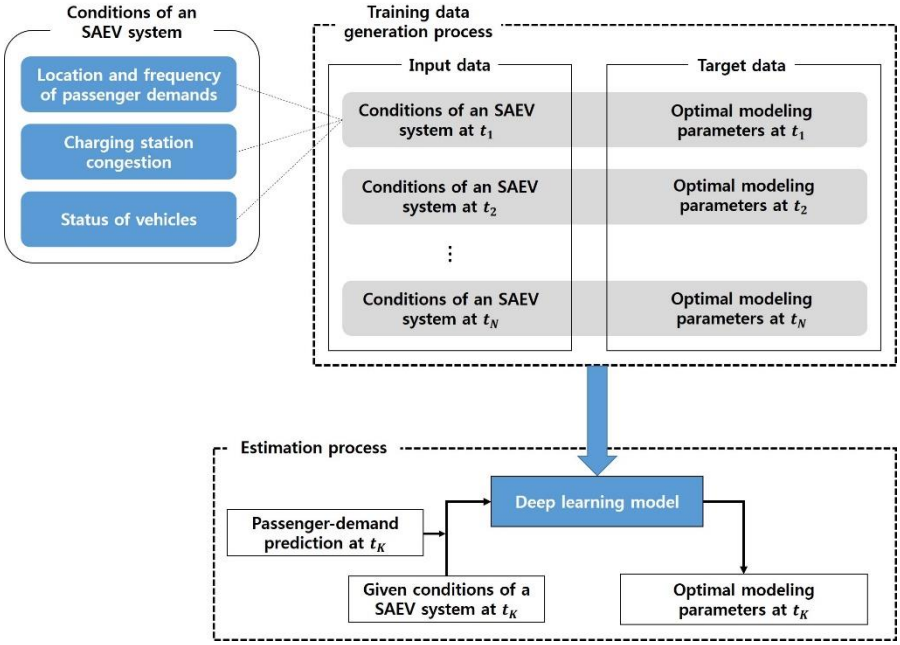

Fig. 6. Flowchart of the real-time prediction model for modeling parameters.

4.3.1. Training Data Generation

The training-data generation process produces input and target data needed for training the real-time prediction model for modeling parameters. Conditions of an SAEV system at a certain moment and corresponding optimal modeling parameters constitute the input and target data, respectively. In this study, real time was assumed to be a 30-min interval. Thus, SAEV simulations were conducted by dividing 24 hours per day into 30-min intervals to obtain training data. Fig. 7 shows an example of input and target data generation performed in a 30-min SAEV simulation at t_i. The conditions of an SAEV system comprise three factors used as the input data: (1) location and frequency of passenger demands for intervals of 30 minutes; (2) charging-station congestion indicating whether the chargers are occupied and when charging ends; and (3) status of vehicles, including current location, remaining battery capacity, and service status. The second and third factors are given at the beginning of the 30-min SAEV simulation. Then, optimal modeling parameters obtained through optimization from 30-min interval SAEV simulations become the target data of the interval. The consideration of three factors in training data allows the trained deep learning model to derive appropriate optimal modeling parameters in real time for given conditions. In this study, training data sets obtained from 30-min SAEV simulations for 363 days were used. Thus, a total of 17424 sets of input and target data were employed. To obtain the optimal modeling parameters from each simulation, a genetic algorithm was used for global search, and sequential quadratic programming was applied for local search. If a special change occurs in the conditions of an SAEV system in the future, then the prediction of optimal modeling parameters may fail. Therefore, continuous accumulation of training data over time and updating of the real-time prediction model are required.

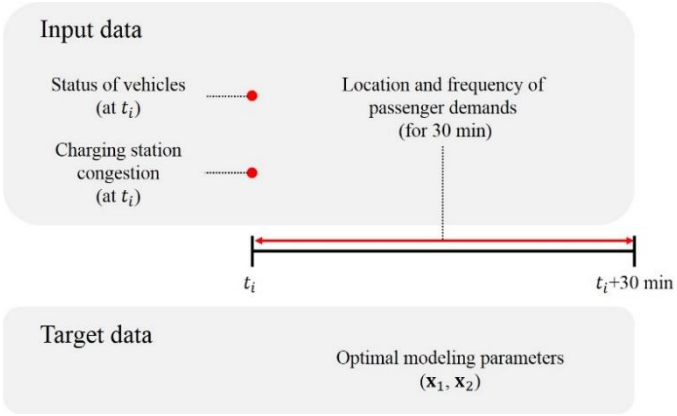

Fig. 7. Example of input and target data generation.

4.3.2. Training

The training data produced as described above were transformed into a 133×112 grid including all the location information to pass through the convolutional layer. This is one tenth of the area of Seoul city. In each channel and 4 channels of the charging station are combined, and 133×112×8 imaged data were used as input. Fig. 8 shows an example of preprocessed data: Fig. 8 (a) shows the passenger demand's location and frequency for an example of 30 minutes; Fig. 8(b) shows the CS congestion indicating whether the chargers are occupied and when the charging ends. Each of the 6 points indicates the charging time of the charger at each of 6 charging stations; Fig. 8(c) shows the SAEV's current location; Fig. 8(d) shows the SAEV's battery capacity; and Fig. 8(e) shows the SAEV's service ending time, which is the time when SAEV drops off customers and moves around in an empty vehicle. The color changes from blue to yellow as each respective indicator increases.

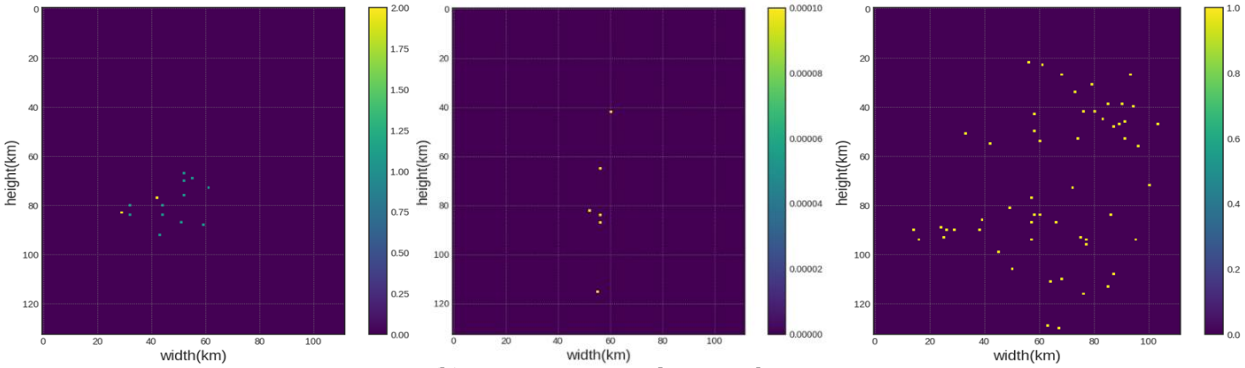

(a) Passenger demand's location and frequency

(b) CS congestion indicating charger occupancy and charging end time (hr)

(c) SAEV's current location

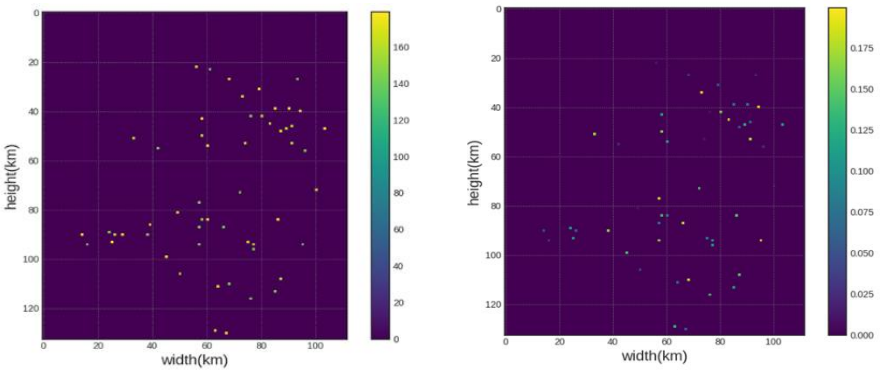

(d) SAEV's battery capacity (kWh)

(e) SAEV's service ending time (hr)

Fig. 8. Example of input data visualization as images.

Four parameter values in total were obtained at the output. Min-max scaling was performed on the input, and the logarithm was taken to increase the normality for target values and to derive meaningful results during regression analysis [39]. The shape of the input data was 133×112×8. Eight channels of 2D images were obtained by performing a pre-processing process that divides Seoul into a grid array of 133 rows × 112 columns every 30 min. In Fig. 3, eight channels refer to eight timeslots of 30 min each; this is an image of a taxi call that occurred for 4 h as dots. The data used for learning in this study are time-series data, which are split using sliding time window. Train-test data are not randomly shuffled. A total of 13839 data, which constitute 80% of 17424 data, were used as the training set, whereas 3484 data (the remaining 20%) were used as the test set. In time-series data, the records in first 289 days data were trained, and the remaining 74 days were tested. These data were not trained with methods, such as LSTM or RNN, but rather with CNN, in consideration of spatial correlation and complex nonlinearity.

In this study, to determine the optimum architecture for mixed input features, we compared the performances of CNN, Unet [38], and GCN [40] architectures. We finally select the CNN-based architecture shown in Fig. 9. The proposed architecture is composed of 6 convolutional layers and batch normalization, 2 max-pooling layers, a ReLu activation function, and the Regressor part, which is composed of 1 fully connected layer and dropout. It was trained using the same Adam optimizer as for the passenger demand prediction model. The learning rate was set to 0.001; decay rate to 0.005; and batch size to 256; further, early stopping was applied. The training took approximately 1 hour with four GPUs (GTX 1080) operating in parallel.

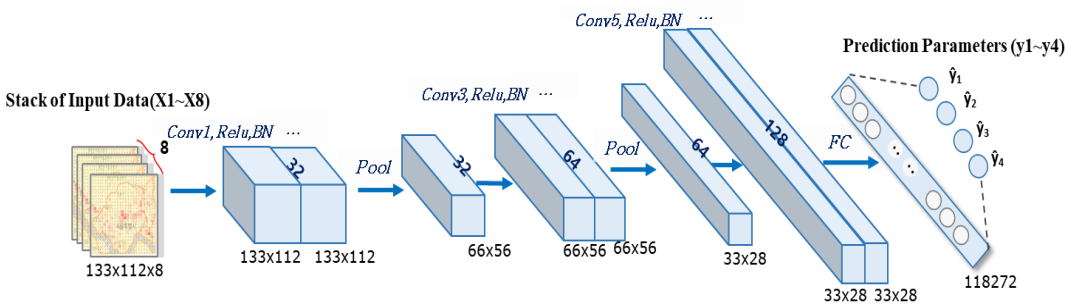

Fig. 9. Deep learning architecture for idle vehicle relocation.

5. Application of SAEV System Optimization

In this study, Seoul was used as a test-bed, and the SAEV system framework presented by Lee et al., which follows a random-motion strategy, was modified to apply the proposed destination selection algorithm to Seoul's data [15]. The SAEV system framework presented in Fig. 10 consists of a fleet operation model, SAEV design model, and CS model. It derives the customer's wait time for a given SAEV system design. The fleet operation model reflects road circumstances to perform shortest-time-path search and determines the optimal fleet assignment by considering the destination selection of vehicles not in service and the charging schedule. The SAEV design model determines the charging time of the battery and EV performance metrics, such as driving range, top speed, acceleration, and miles per gallon equivalent (MPGe). Finally, the CS model determines the optimal locations of CSs and the total number of chargers. In this study, fleet operation is assumed to be performed by a central operating system that manages passenger demands, destination selections, and status of EVs and CSs.

Real road connections and CS locations in Seoul are shown in Fig. 11 and the determination of CS locations is explained in Section 5.2. The crossing points and connections of roads are respectively set as nodes and segments to represent real roads. The test-bed represents the roads of Seoul with a total of 463 nodes and 845 segments.

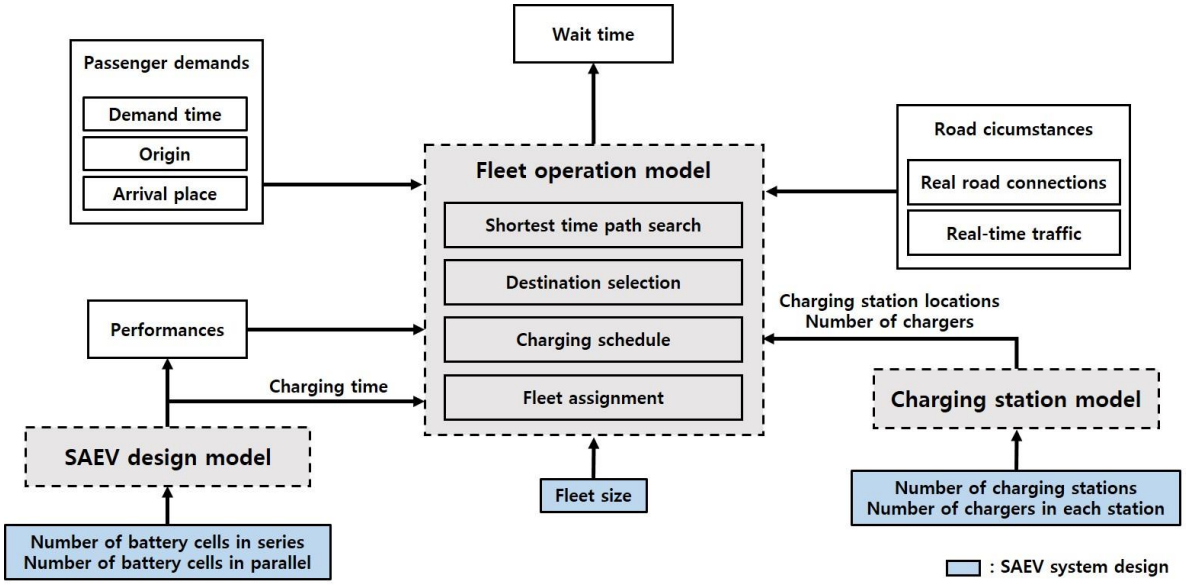

Fig. 10. SAEV system framework.

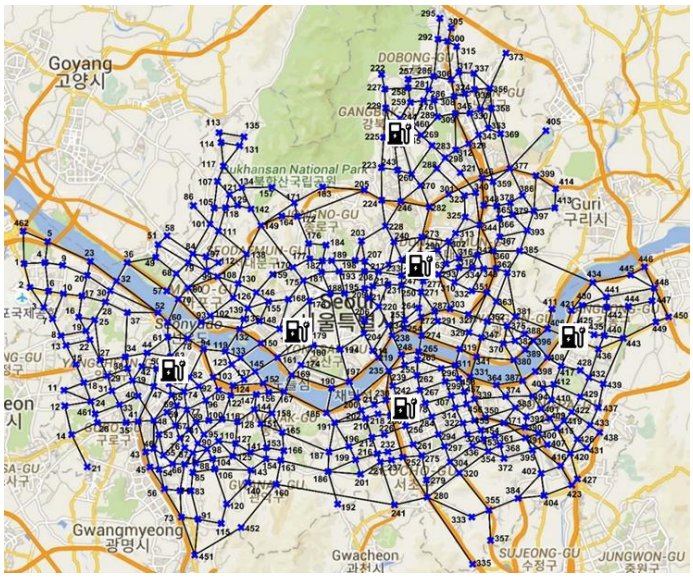

Fig. 11. Real road connections and CS locations in Seoul.

5.1. Fleet Operation Model

The fleet operation model determines the optimal fleet assignment according to passenger demands and provides customer's wait time as the output. In the fleet operation of an SAEV, the fleet can have the following three states: (1) idle, in which the vehicle is not in service and moves to the selected destination where passenger demands are expected to occur; (2) in-service, in which the vehicle is assigned to a customer and is occupied; and (3) charging, in which the battery is charged when the state-of-charge (SOC) of the battery falls below a certain level. The flowchart of the fleet operation model for 24 h is presented in Fig. 12. The initial vehicle information for each day, including the vehicle location, the SOC of the battery, and the time when the vehicle service ends and its state becomes idle, was set randomly. In the idle state, the fleet moved to the destination according to the proposed idle vehicle relocation strategy. In the fleet, a candidate vehicle can be assigned to the customer when a passenger demand occurs along the route. The central operating system continuously monitored the SOC of the battery during the idle state. It instructed the vehicle to go to a CS when the SOC of the battery reached a certain level. If empty chargers existed, then the nearest charger was assigned. The charger with minimum wait time was assigned in case all chargers in the CSs were occupied. The central operating system managed the charging

schedule by monitoring the start and end times of charging of each charger. When a passenger demand occurred, a vehicle with feasible SOC went to the nearest CS after the service was included in the candidate vehicles, and a vehicle that minimized the customer wait time was selected to carry out the service. After service, the SOC of the battery was checked, and the vehicle started its idle or charging state.

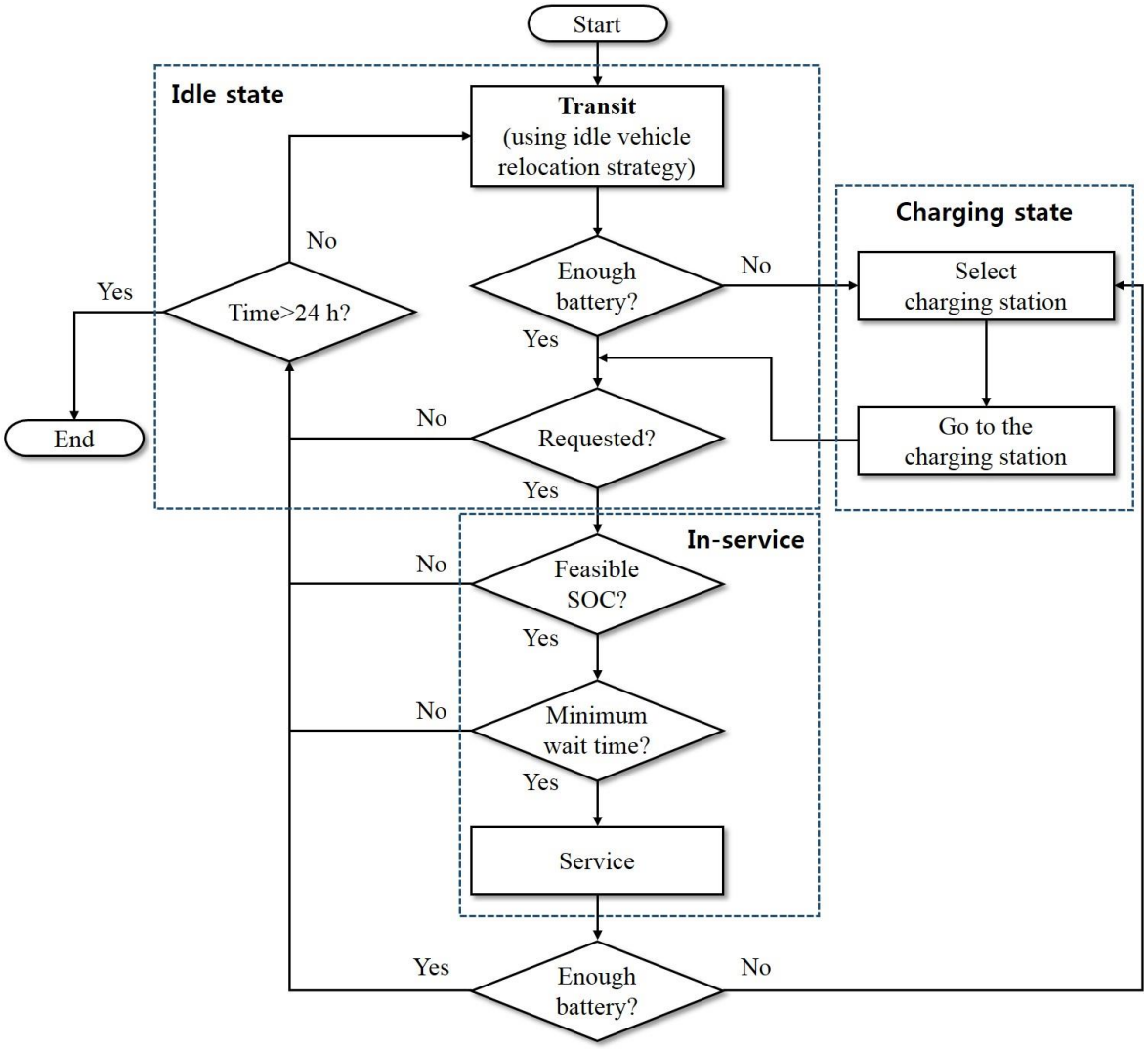

Fig. 12. Flowchart of the fleet operation model.

When the SAEV moved from one place to another, it moved along the shortest time path derived from the shortest path algorithm proposed by Dijkstra [41]. The shortest time path was obtained by considering the traffic of each road section in real time. The real-time traffic was applied to the shortest path algorithm by considering the distance of each road section differently depending on the average speed of each road section. If the average speed of the road section was lower than the average speed of Seoul roads (35.8 km/h), then the shortest path algorithm recognized the longer distance of the road section with respect to the actual distance and derived the shortest path that can be regarded as the shortest time path. To reflect the real-time traffic of Seoul, the real-time average speed data of Seoul roads provided by the Seoul Metropolitan Government were used as the average speed of each road section [42]. The average speed of road sections over time is summarized in Table 2. The traffic flow was smooth at dawn and was heavy during rush hour. When moving, an SAEV was assumed to move with real-time average speed in each road section

Table 2. Average speed of road sections over time.

Time	0–30 km/h (%)	30–60 km/h (%)	60–90 km/h (%)	90–120 km/h (%)	Average speed (km/h)
0:00–1:00	36.92	44.85	15.74	2.49	41.2

1:00–2:00	24.38	56.45	14.20	4.97	44.1
2:00–3:00	16.09	64.50	14.20	5.21	46.0
3:00–4:00	10.76	68.88	15.27	5.09	47.4
4:00–5:00	11.36	67.93	15.62	5.09	47.3
5:00–6:00	19.53	60.82	15.86	3.79	44.8
6:00–7:00	30.53	53.61	15.62	0.24	40.6
7:00–8:00	46.86	41.30	11.72	0.12	36.3
8:00–9:00	60.83	29.35	9.70	0.12	33.4
9:00–10:00	60.95	29.23	9.70	0.12	33.3
10:00–11:00	61.30	29.35	9.23	0.12	32.7
11:00–12:00	62.01	28.88	8.87	0.24	32.7
12:00–13:00	60.35	28.05	11.36	0.24	33.6
13:00–14:00	61.18	27.81	10.77	0.24	32.8
14:00–15:00	64.26	27.10	8.52	0.12	31.2
15:00–16:00	65.91	26.15	7.81	0.12	30.4
16:00–17:00	66.62	26.51	6.75	0.12	29.4
17:00–18:00	71.01	23.31	5.68	0.00	27.4
18:00–19:00	74.20	22.49	3.31	0.00	26.0
19:00–20:00	69.47	26.51	4.02	0.00	28.3
20:00–21:00	61.06	27.93	11.01	0.00	32.5
21:00–22:00	57.04	29.82	13.02	0.12	34.4
22:00–23:00	54.20	32.31	13.25	0.24	35.1
23:00–24:00	46.86	37.16	14.91	1.07	38.1

Some details and information about the fleet operation model are provided as follows:

1. The passenger demand data, including the passenger demand time, origin, and arrival place, are generated upon the Seoul taxi data provided by the Seoul Metropolitan Government [37].
2. The central operating system is assumed to receive the passenger demand data of the customer in real time through their smartphone app.
3. If the origin or arrival place submitted by the customer is not exactly on the node, then the SAEV is assumed to move to the closest node toward the request point. Then, the SAEV gets out of the segment (road) to reach the request point.
4. An SAEV moves in fully autonomous driving mode along the shortest time path.

5.2. SAEV Design and CS Models

The SAEV design and CS models provide vehicle performance and CS information to the fleet operation model, respectively, thereby predetermining the SAEV and CS design to explore and develop the destination selection algorithm effectively. The SAEV design model uses the EV simulation model presented by Lee et al. to determine the vehicle performance metrics, such as range, MPGe, acceleration (0−100), and top speed [43]. The EV simulation model reflects the vehicle's powertrain design, and the gear ratio is assumed to be 8.2, as in Nissan Leaf [44]. The number of battery cells in the series determines the voltage of the battery, which in turn affects acceleration and top speed. The number of battery cells in parallel affects the range by determining the battery capacity.

The CS model determines the capacity of the CSs by providing CS locations and number of chargers to the fleet operation model. The SAEV simulation was performed on the basis of approximately 1000 customers per day, and six CSs with four chargers in each station were assumed to be adequate to handle them. Government-operated CSs in Seoul are used as candidates for CS locations [45]. Among candidates, six CS locations shown in Fig. 11, namely, node numbers 64,173, 251, 268, 424, and 459, were determined using the *p*-median model that minimizes the path distance between any node and its closest CS [46]. The capacity of the CSs determines the CS wait time, which is the time that an SAEV should wait to charge in the case all chargers of the CSs are in use. This affects the customer wait time in the SAEV simulations. Each charger uses a direct-current fast charging system that charges a 24-kWh battery in 30 min.

Prior to SAEV system optimization in Section 5.3, the candidates of CS locations are pre-determined using the *p*-median model. Given that the number of CSs is prescribed, the node numbers of the CSs in Fig. 11 are determined according to Table 3.

Table 3. Candidates of CS locations.

Number of CSs	Candidates of CS locations (node numbers)
1	206
2	64,173
3	64,173,268
4	64,173,268,424
5	64,173,251,268,424
6	64,173,251,268,424,459
7	64,173,193,251,268,424,459
8	64,173,193,203,251,268,424,459
9	64,173,193,203,251,268,379,424,459
10	9,64,173,193,203,251,268,399,424,459
11	9,64,173,193,203,208,251,268,399,424,459
12	9,64,173,193,203,206,208,251,268,399,424,459
13	9,64,173,193,203,206,208,251,268,399,424,456,459
14	9,64,173,193,203,206,208,251,268,379,399,424,456,459
15	9,64,153,173,193,203,206,208,251,268,379,399,424,456,459

5.3. Formulation of SAEV System Optimization

A seven-day simulation was conducted for the SAEV system optimization problem that minimizes the cost while satisfying the customer's wait time constraint, and the results are discussed in Section 6.2. In the seven-day simulation, we assumed that an SAEV occupies a part of the traditional transportation system and on average 942 customers use the SAEV service per day. The customer's passenger demand time, origin, and arrival place in the simulation were generated upon the passenger demand data of Seoul. The number of customers per day was appropriately determined considering the time required for simulation. The optimization problem for the design of the SAEV system is formulated as follows [15]:

$$
\begin{aligned}
\text{find} \quad & \mathbf{X}=\left[N_{\text{CS}}, N_{\text{charger}}, N_{\text{SAEV}}, \mathbf{X}_{batt}^{\text{T}} \right] \\
\min_{\mathbf{X}} \quad & \text{Cost}(\mathbf{X}) \\
\text{subject to} \quad & \mathbf{lb} \le \mathbf{X} \le \mathbf{ub} \\
& \text{g}_{\text{SAEV}}(W) \le 0 \\
\text{where} \quad & \mathbf{X}_{batt}=\left[N_{\text{S}}, N_{\text{P}} \right]^{\text{T}} \\
& \left[P_{\text{range}}, T_{\text{charging}} \right] = f_{\text{SAEV}}\left(\mathbf{X}_{batt} \right) \\
& \left[\mathbf{L}_{\text{CS}}, C_{\text{CS}} \right] = f_{\text{CS}}\left(N_{\text{CS}}, N_{\text{charger}} \right) \\
& \left[W, C_{\text{SAEV}} \right] = f_{\text{operation}}\left(N_{\text{SAEV}}, \mathbf{L}_{\text{CS}}, N_{\text{charger}}, P_{\text{range}}, T_{\text{charging}} \right),
\end{aligned}
\tag{2}
$$

where the objective of the problem is to minimize the cost, consisting of CS and SAEV fleet costs; **X** is a decision variable vector; N_{CS}, N_{charger}, and N_{SAEV} are the numbers of CSs and chargers per each CS, and the SAEV fleet size, respectively; $\mathbf{X}_{batt}$ indicates the battery design variable vector; **lb**, **ub**, and g are the lower and upper bounds, and the customer's wait time constraint, respectively; W is the mean customer's wait time, whose constraint was set such that W satisfies 5 minutes; N_{S} and N_{P} are the numbers of battery cells in series and parallel, respectively; P_{range} and T_{charging} are the driving range and charging time of an SAEV, respectively; $\mathbf{L}_{\text{CS}}$ denotes the CS location vector; C_{CS} is the CS cost encompassing the installment and maintenance of CSs; C_{SAEV} is the SAEV fleet cost; and f_{SAEV}, f_{CS}, and $f_{\text{operation}}$ indicate the SAEV design, CS, and fleet operation models, respectively. Before starting the optimization, the candidates for CS locations are pre-determined using a *p*-median model as shown in Section 5.2. The wait time constant restricts the customer's wait time for the wait to be short. Thus, it is assumed that all customers use the SAEV service. The SAEV system optimization results are determined to handle the given customer demand.

An SAEV incurs the following costs: lithium-ion battery, \$236/kWh [47]; autonomous module, \$10,000 [12]; 80-kW permanent magnet synchronous motor, \$1,665 [48]; other costs for the vehicle, assumed to be \$6,000. The installment and maintenance costs of each charger in CS are assumed to be \$22,626 and \$5,000, respectively [12,49].

6. Simulation Results

6.1. Results of Idle Vehicle Relocation Strategy

6.1.1. Deep learning-based Demand Prediction

Concerning performance metrics, the passenger demand prediction, root mean square error (RMSE), and mean absolute percentage error (MAPE) were used. The results are summarized in Table 4. SEO-Taxi is the Seoul taxi vendor data set provided by Seoul City used after preprocessing. When weather data were used in SEO-Taxi data, the performance in terms of RMSE and MAPE was improved by 6.3% and 5.1%, respectively. For reference, the results for the Seoul-rite-hailing datasets of Kakao taxi used by TGNet have RMSE and MAPE of 25.35 and 35.72%, respectively.

Table 4. Comparison of forecasting results on SEO-Taxi and SEO-Taxi with external data for TGNet model.

Method	SEO-Taxi		SEO-Taxi with external data	
	RMSE	MAPE (%)	RMSE	MAPE (%)
TGNet	3.90	33.20	3.67	**31.60**

6.1.2. Idle Vehicle Relocation by Optimization

This section presents the optimization results of modeling functions and parameters constituting the destination selection algorithm explained in Section 4.2. The optimization results are compared in terms of the mean wait time of customers obtained from the seven-day simulation presented in Section 5. In the simulation, the SAEV system design was assumed to accommodate the given number of customers per day: the number of fleets was 63; number of charging stations and chargers in each station were 6 and 4, respectively; number of battery cells in series and parallel were 110 and 2, respectively; and gear ratio was 8.2. The range, MPGe, acceleration, and top speed obtained from the given SAEV design are 179.3 km, 135.9, 10.1 s, and 150.5 km/h, respectively. For the purpose of comparison, the mean wait time results obtained using a random-motion strategy, which was frequently applied in previous SAEV studies, were employed as benchmarks. The results are summarized in Table 5.

Table 5. Mean wait time results obtained using a random-motion strategy (minutes).

Day 1	Day 2	Day 3	Day 4	Day 5	Day 6	Day 7
11.90	11.69	10.44	11.03	11.49	12.76	12.45

Table 6 summarizes the optimal parameters and mean wait time results according to the modeling function type. The given modeling function type was equally applied to f_1 and f_2, and the optimization problem expressed by Eq. (1) was solved for each day (24 hours) to derive optimal parameters. For optimization of this 24-h interval simulation, a genetic algorithm was used for global search, and sequential quadratic programming was used for local search. The computation time for one optimization was 4 hours on average using a standard desktop computer (Intel Xeon 8168 CPU @ 2.70 GHz with 192.0 GB of RAM).

Table 6. Optimization results depending on the modeling function type.

	Modeling function type	f_1		f_2		Mean wait time (minutes)
		x_1	x_2	x_3	x_4	
Day 1	Linear	0.1007	-	1.4064	-	3.24
	Concave	0.0458	1.2487	0.3251	9.6157	3.22
	Exponential-Gauss	0.1059	1.5015	3.0336	2.6666	3.16
Day 2	Linear	0.0969	-	1.4650	-	3.01
	Concave	0.0034	2.3840	6.2043	3.7056	3.02
	Exponential-Gauss	0.0145	2.3180	3.6977	2.1203	2.95
Day 3	Linear	0.1598	-	0.4219	-	2.58

	Concave	0.0047	2.9645	0.1526	4.2942	2.57
	Exponential-Gauss	0.3978	1.0491	0.9246	1.5538	2.54
Day 4	Linear	0.1025	-	0.9983	-	2.81
	Concave	0.0185	1.7005	5.6648	8.6433	2.80
	Exponential-Gauss	0.0488	2.2345	1.7868	1.3224	2.76
Day 5	Linear	0.0930	-	0.9634	-	2.88
	Concave	0.0115	1.9886	0.8139	5.6652	2.87
	Exponential-Gauss	0.1656	1.2461	2.1201	2.1727	2.85
Day 6	Linear	0.0687	-	2.1172	-	4.27
	Concave	0.0518	1.0867	7.9813	5.3493	4.16
	Exponential-Gauss	0.0683	1.8004	4.9477	0.7728	4.16
Day 7	Linear	0.0893	-	2.5576	-	3.62
	Concave	0.0088	1.7094	2.0491	2.1507	3.59
	Exponential-Gauss	0.0246	1.9897	0.5280	3.1947	3.55

For all modeling function types, the mean wait time obtained from the simulation using the destination selection algorithm with optimized parameters was considerably reduced with respect to the simulation using a random-motion strategy—the mean wait time was reduced by 72.73% (8.46 minutes), 72.93% (8.50 minutes), and 73.29% (8.54 minutes) on average when using the linear, concave, and exponential-Gauss functions, respectively. This shows that the destination selection algorithm properly selects the destination of the idle-state SAEV and efficiently performs the fleet operation. The mean wait time varied depending on the modeling function type—the mean wait time was 3.20 minutes, 3.18 minutes, and 3.14 minutes on average when using the linear, concave, and exponential-Gauss functions, respectively. This indicates that nonlinear functions describe the probability of selection better than a simple linear function. In addition, the exponential-Gauss function is more suitable than the concave function for modeling. This was confirmed in all seven-day simulations. As a result of performing optimization in a situation where the modeling function types of f_1 and f_2 can be different, the optimal modeling functions for both f_1 and f_2 were exponential-Gauss throughout the seven days. The results also demonstrate that the optimal parameters of the modeling function were different for each day, which means that the optimal parameters vary according to the conditions of a given SAEV system.

To analyze the characteristics of f_1 and f_2, function value comparison for the same O_{ij}—distance from the current location to the destination for f_1 and vehicle excess at the destination for f_2—was performed. The average function value for 7 days is presented in Table 7. The f_1 gradually decreases with increasing distance to the destination, whereas f_2 rapidly decreases when vehicle excess occurs and converges to 0 when vehicle excess increases. This finding verifies that the passenger demand prediction model is well applied to the destination selection algorithm. The model avoids the assignment of idle vehicles to locations where the number of vehicles already assigned exceeds the expected customer demand.

Table 7. Function value comparison for the same O_{ij}.

	$O_{ij}=1$	$O_{ij}=2$	$O_{ij}=3$	$O_{ij}=4$	$O_{ij}=5$
f_1	0.8952	0.7536	0.5990	0.4508	0.3235
f_2	0.1934	0.0123	0.0009	0.0000	0.0000

Sensitivity analysis for the probability of selection was performed to determine how P_1, P_2, and P_3 affect the destination selection algorithm. The exponential-Gauss function with optimal parameters was used for f_1 and f_2. The mean wait time results that depend on the combination of probability of selection are summarized in Table 8. In the simulations, the destination selection algorithm selects a destination after considering the given combination of the probability of selection. When only P_1 is considered, the mean wait time is reduced by 59.71% (6.97 min) on average with respect to the application of the random-motion strategy, thereby indicating that the P_1 provided by the passenger demand prediction model has a significant impact on the reduction of the customer wait time. Compared with the case where only P_1 is considered, the mean wait time is reduced by 17.33% (0.79 min) and 25.4% (1.17 min) on average in cases where P_1 and P_2 are considered and where P_1 and P_3 are considered, respectively. The P_3 is relatively more important than P_2 in the destination selection algorithm. Predicting the vehicle excess at the destination accurately and assigning the appropriate number of SAEVs to each destination are important. When all P_1, P_2, and P_3 are considered, the mean wait time is reduced by 33.83% (1.58 min) on average compared with when only P_1 is considered. Thus, it is important to consider both the distance from the current location to the destination and the vehicle excess at the destination.

Table 8. Mean wait time results depending on the combination of probability of selection (minutes).

Combination of probability of selection	Day 1	Day 2	Day 3	Day 4	Day 5	Day 6	Day 7
P_1	4.68	4.51	4.23	4.39	4.43	5.68	5.07
$P_1 \times P_2$	4.17	3.77	3.06	3.43	3.51	5.20	4.31
$P_1 \times P_3$	3.56	3.30	2.78	3.12	3.14	4.78	4.11
$P_1 \times P_2 \times P_3$	3.16	2.95	2.54	2.76	2.85	4.16	3.55

6.1.3. Idle Vehicle Relocation by Deep Learning

To evaluate the performance of the deep learning model, we used both RMSE and mean absolute error (MAE) as evaluation metrics. The RMSE and MAE for the test data were 1.25 and 0.93, respectively. To demonstrate the performance of the modeling parameter prediction model for real-time operation, the mean wait time results obtained by optimizing modeling parameters from 30-min interval simulations were used as benchmarks. The mean wait time and optimal modeling parameter results from seven-day simulations—each day's simulation consisting of 48 30-min simulations—are summarized in Table 9. As in Section 6.1.2, a genetic algorithm was used for global search, and sequential quadratic programming was applied for local search. The mean wait time obtained by optimizing modeling parameters from 30-min interval simulations was reduced by 21.07% (0.7 minutes) on average compared to that of the 24-h interval simulation. This indicates that it is important to provide optimal modeling parameters for each short interval simulation given that the optimal values change continuously depending on the given conditions of an SAEV system. The large standard deviation of optimal parameters also shows that the optimal parameters change significantly for every 30-min interval simulation. This stresses the need for an alternative method to optimization that promptly provides optimal modeling parameters, as it is difficult to complete optimization in a short time.

Table 9. Mean wait time and optimal parameter results from 30-min interval simulation (obtained through optimization).

	f_1		f_2		Mean wait time (minutes)
	x_1	x_2	x_3	x_4	
Day 1	1.2889 (1.1798)*	0.9365 (0.9041)	2.6879 (1.5383)	2.6654 (1.4913)	2.44
Day 2	1.7521 (1.3620)	1.1572 (1.1367)	2.8835 (1.3148)	2.7875 (1.4591)	2.32
Day 3	2.1739 (1.5006)	1.6720 (1.5035)	2.4483 (1.5440)	2.0584 (1.2894)	2.23
Day 4	1.2818 (1.2234)	1.2396 (1.2750)	2.6553 (1.5672)	2.4479 (1.4271)	2.33
Day 5	1.4679 (1.2103)	1.2077 (1.1902)	2.9140 (1.4210)	2.3957 (1.3621)	2.41
Day 6	1.5970 (1.5075)	0.9752 (1.1637)	2.6074 (1.3903)	2.2495 (1.4581)	2.76
Day 7	0.9561 (0.9634)	0.9870 (1.1010)	2.6718 (1.4152)	2.4123 (1.5566)	2.60

*Standard deviations are enclosed in parentheses

The modeling parameter prediction model for real-time operation provides optimal modeling parameters according to given conditions of an SAEV system every 30 minutes. The mean wait time and optimal modeling parameters are presented in Table 10. They were obtained from a seven-day simulation through 30-min intervals performed with optimal modeling parameters provided by the modeling parameter prediction model. When using such model instead of optimization, the mean wait time was increased by 5.40% (0.13 minutes) on average, but it was reduced by 77.97% (9.10 minutes) on average with respect to applying a random-motion strategy. This shows that the decrease in the customer's wait time was still significant when using the modeling parameter prediction model. This also indicates that the modeling parameter prediction model provides appropriate parameters

according to the given SAEV system condition. The difference between the parameters provided by such model and the parameters obtained through optimization can be explained by the error generated in the predicted location and frequency of passenger demands, which are provided by the passenger demand prediction model and used as input data of the modeling parameter prediction model. To further justify the competitiveness of the modeling parameter prediction model, the mean wait time results derived with sub-optimal solutions, which are obtained by limiting the time of the optimization algorithm, are shown in Table 11. Considering the time limit in real-time optimization, the time limit was set to 1 s. Compared with when using the time-limited optimization, the mean wait time was reduced by 16.59% (0.51 min) on average when the modeling parameter prediction model was used. This indicated the rationality of using the modeling parameter prediction model in real practice. When the results obtained using the modeling parameter prediction model are compared with those obtained using the time-limited optimization, the following results can be obtained: the response time decreases by 17.37% (0.35 min); the overall fleet distance decreases by 0.74% (2,415 km); and the deadheading distance per day decreases by 1.05% (345 km). If the constraint that the customer uses the service when the wait time is less than 6 minutes is given, the percentages of demand served obtained by using the modeling parameter prediction model and the time-limited optimization are 95.26% and 91.73%, respectively. The percentages of deadheading distance for relocation are 65.81% and 65.98% when using the modeling parameter prediction model and the time-limited optimization, respectively. These results verify that using the modeling parameter prediction model increases the efficiency of fleet operation compared to using time-limited optimization. In addition, sensitivity analysis according to the time limit of the time-limited optimization was performed. When the time limit was increased from 1 s to 2 s, the mean wait time decreased by 0.078 s on average. When a special situation occurs for the first time, the modeling parameter prediction model may fail to predict optimal modeling parameters. In this case, if the simulation interval is large enough compared to the optimization time, optimization can yield better solutions than the modeling parameter prediction model; however, if the time required for optimization is larger than the simulation interval, optimization cannot guarantee accurate optimal solutions as in time-limited optimization.

Table 10. Mean wait time and optimal parameter results from 30-min interval simulation (using the modeling parameter prediction model).

	f_1		f_2		Mean wait time (minutes)
	x_1	x_2	x_3	x_4	
Day 1	0.9964 (0.5149)*	0.7899 (0.4564)	1.7234 (0.8806)	2.0064 (0.7399)	2.56
Day 2	1.2114 (0.6982)	0.8852 (0.4664)	1.9380 (0.9750)	1.6121 (0.7479)	2.48
Day 3	1.2288 (0.6687)	0.9018 (0.4693)	1.7609 (0.7822)	1.7782 (0.7563)	2.30
Day 4	1.1217 (0.6847)	0.7963 (0.6451)	1.9193 (0.9745)	1.9347 (0.7885)	2.41
Day 5	0.9873 (0.5378)	0.7337 (0.4624)	2.0396 (0.9936)	1.9675 (0.9201)	2.55
Day 6	0.9960 (0.5110)	0.8238 (0.4729)	2.1468 (0.9536)	2.1951 (0.9066)	2.97
Day 7	0.9964 (0.5149)	0.7899 (0.4564)	1.7234 (0.8806)	2.0064 (0.7399)	2.76

*Standard deviations are enclosed in parentheses

Table 11. Mean wait time results from 30 min interval simulation obtained using time-limited optimization (minutes).

Day 1	Day 2	Day 3	Day 4	Day 5	Day 6	Day 7
3.12	3.06	2.79	2.96	2.98	3.29	3.41

6.2. Results of SAEV System Optimization

Table 12 summarizes optimal designs and outcomes obtained from Eq. (2) where the destination selection algorithm using the modeling parameter prediction model for real-time operation is applied. The results are

compared with those obtained using a random-motion strategy. When using the destination selection algorithm, the cost was reduced by 38.2% with respect to applying the random-motion strategy, demonstrating that the destination selection algorithm and modeling parameter prediction model for real-time operation work well. Owing to the modeling parameter prediction model, which provides optimal modeling parameters immediately according to the given conditions of an SAEV system, the destination selection algorithm can be successfully applied to the optimization problem. Through the modeling parameter prediction model, the optimal modeling parameters required in the destination selection algorithm can be provided in real time. Thus, the destination of the idle-state SAEV is properly selected and the efficiency of the fleet operation can be increased. This results in reduction in the fleet size and the number of charging stations required to satisfy the wait time constraint. In addition, the destination selection algorithm reduces the average daily driving distance of a vehicle by increasing the fleet operation efficiency. The average daily driving distance of a vehicle is 844.2 and 780.8 km when the random-motion strategy and the destination selection algorithm are used, respectively. The destination selection algorithm reduces the time by which vehicles stay on the road and the fleet size required to satisfy the wait time constraint, thereby reducing overall congestion.

Table 12. Optimal designs and outcomes of the SAEV system optimization problem with wait time constraint.

		Random-motion strategy	Destination selection algorithm
Decision variables	Fleet size	75	50
	Number of CSs	9	6
	Location of CSs	64,173,193,203,251,268, 379,424,459	64,173,251,268,424,459
	Number of chargers	3	2
	Number of battery cells in series	101	139
	Number of battery cells in parallel	1	1
Vehicle spec.	Acceleration (0–100)	10.3 s	8.5 s
	Range	84.3 km	115.3 km
	Top speed	148.2 km/h	158.2 km/h
	MPGe	140.0	138.5
	Battery capacity	12.7 kWh	17.5 kWh
Cost	Total cost	$2,309,134	$1,427,066
	Fleet cost	$1,549,731	$1,089,554
	CS installment cost	$610,903	$271,512
	CS maintenance cost	$148,500	$66,000
Fleet operation	Charging time	13.5 minutes	18.6 minutes
Customer’s wait time	Mean	4.99 minutes	4.94 minutes

7. Conclusion

This study proposes a deep learning-based idle vehicle relocation strategy that decides the location of the idle SAEV in real time. The proposed idle vehicle relocation strategy is achieved through 3 steps. In Step 1, a deep learning-based prediction model is built to forecast the location and frequency of passenger demand. Interestingly, weather information is added to TGNet as supplemental data to improve the performance. In Step 2, a relocation optimization algorithm decides the idle vehicle destinations based on passenger demand prediction. Three probability distributions are defined for relocation strategy and for setting optimal modeling parameter values for training. In Step 3, a deep learning model estimates the optimal modeling parameters without optimization process. By introducing modeling parameters that have different optimal values depending on the conditions of SAEV system, optimal idle vehicle relocation can be performed flexibly for various conditions of SAEV system.

The proposed idle vehicle relocation strategy was also applied to the SAEV system optimization problem, and the performance of the modeling parameter prediction model for real-time operation was investigated. The proposed idle vehicle relocation strategy reduced the cost by 38.2% with respect to applying a random-motion strategy. The relocation algorithm makes efficient automobile operation CS possible and reduces the number of charging stations and automobile size needed to fulfill the wait time limit. These results confirm that the proposed

algorithm operates well for on-demand service. Through the idle vehicle relocation strategy proposed in this study, efficient fleet operation becomes possible even with a small fleet size, which can help reduce traffic congestion. This study can be considered as a stepping stone for introducing deep learning into SAEV fleet operation. In addition, this study can be applied to various on-demand services that require real-time operation, reducing customer wait time and operating cost.

Concerning future work, we plan to focus on improving the accuracy of modeling parameter prediction by taking into account various conditions, such as CS congestion and vehicle condition, and location and frequency of travel-request passenger demand, which will be used as training data for modeling parameter prediction models.

Declaration of Competing Interests

The authors declare that they have no known competing financial interests or personal relationships that could have influenced the work reported in this study.

Acknowledgments

This study was supported by National Research Foundation of Korea (NRF) grants funded by the Korean government [grant numbers 2017R1C1B2005266 and 2018R1A5A7025409] and Energy Cloud R&D Program through the National Research Foundation of Korea (NRF) funded by the Ministry of Science, ICT (No. 2019M3F2A 1072468). This study was also supported by HPC Support Project of the Ministry of Science and ICT and NIPA,

References

[1] Loeb B, Kockelman KM. Fleet performance and cost evaluation of a shared autonomous electric vehicle (SAEV) fleet: A case study for Austin, Texas. Transp Res Part A Policy Pract 2019;121:374–385.

[2] Iacobucci R, McLellan B, Tezuka T. Optimization of shared autonomous electric vehicles operations with charge scheduling and vehicle-to-grid. Transp Res Part C Emerg Technol 2019;100:34–52.

[3] Zhang D, Yu C, Desai J, Lau HYK, Srivathsan S. A time-space network flow approach to dynamic repositioning in bicycle sharing systems. Transp Res Part B Methodol 2017;103:188–207.

[4] Chen Z, He F, Yin Y, Du Y. Optimal design of autonomous vehicle zones in transportation networks. Transp Res Part B Methodol 2017;99:44–61.

[5] Meyer J, Becker H, Bösch PM, Axhausen KW. Autonomous vehicles: The next jump in accessibilities? Res Transp Econ 2017;62:80–91.

[6] Moreno AT, Michalski A, Llorca C, Moeckel R. Shared autonomous vehicles effect on vehicle-km traveled and average trip duration. J Adv Transp 2018;2018:10.

[7] Energy Saver. Saving money with electric vehicles. U.S. Department of Energy, https://www.energy.gov/energysaver/articles/saving-money-electric-vehicles; 2015 [accessed 9 March 2020].

[8] Fiori C, Ahn K, Rakha HA. Power-based electric vehicle energy consumption model: Model development and validation. Appl Energy 2016;168:257–268.

[9] Gao Z, LaClair T, Ou S, Huff S, Wu G, Hao P, Barth M. Evaluation of electric vehicle component performance over eco-driving cycles. Energy 2019;172:823–839.

[10] Karabasoglu, O., & Michalek, J. (2013). Influence of driving patterns on life cycle cost and emissions of hybrid and plug-in electric vehicle powertrains. *Energy policy*, *60*, 445-461.

[11] Chen TD, Kockelman KM, Hanna JP. Operations of a shared, autonomous, electric vehicle fleet: Implications of vehicle & charging infrastructure decisions. Transp Res Part A Policy Pract 2016;94:243–254.

[12] Kang N, Feinberg FM, Papalambros PY. Autonomous electric vehicle sharing system design. J Mech Des 2017;139:011402.

[13] Farhan J, Chen TD. Impact of ridesharing on operational efficiency of shared autonomous electric vehicle fleet (No. 18-05821), 2018.

[14] Zhao D, Li X, Cui J. A simulation-based optimization model for infrastructure planning for electric autonomous vehicle sharing. Comput-Aided Civil Infrastruct Eng 2019;1–19.

[15] Lee U, Kang N, Lee I. Shared autonomous electric vehicle design and operations under uncertainties: A reliability-based design optimization approach. Struct Multidiscip Optim 2020;61:1529–1545.

[16] Fagnant DJ, Kockelman KM, Bansal P. Operations of shared autonomous vehicle fleet for Austin, Texas, market. Transp Res Rec 2015;2563:98–106.

[17] Herbawi W, Knoll M, Kaiser M, Gruel W. An evolutionary algorithm for the vehicle relocation problem in free floating carsharing. In *2016 IEEE Congress on Evolutionary Computation (CEC)*, 2016, July, pp. 2873–2879.

[18] Balac M, Ciari F, Axhausen KW. Modeling the impact of parking price policy on free-floating carsharing: Case study for Zurich, Switzerland. Transp Res Part C Emerg Technol 2017;77:207–225.

[19] Loeb B, Kockelman KM, Liu J. Shared autonomous electric vehicle (SAEV) operations across the Austin, Texas network with charging infrastructure decisions. Transp Res Part C Emerg Technol 2018;89:222–233.

[20] Phithakkitnukoon S, Veloso M, Bento C, Biderman A, Ratti C. Taxi-aware map: Identifying and predicting vacant taxis in the city. In *International Joint Conference on Ambient Intelligence*, 2010, November, pp. 86–95, Springer.

[21] Yuan J, Zheng Y, Zhang L, Xie X, Sun G. Where to find my next passenger. In *Proceedings of the 13th International Conference on Ubiquitous Computing*, 2011, September, pp. 109–118.

[22] Li B, Zhang D, Sun L, Chen C, Li S, Qi G, Yang Q. Hunting or waiting? Discovering passenger-finding strategies from a large-scale real-world taxi dataset. In *2011 IEEE International Conference on Pervasive Computing and Communications Workshops (PERCOM Workshops)*, 2011, March, pp. 63–68.

[23] Zhang J, Zheng Y, Qi D, Li R, Yi X. DNN-based prediction model for spatio-temporal data. In *Proceedings of the 24th ACM SIGSPATIAL International Conference on Advances in Geographic Information Systems*, 2016, October, pp. 1–4.

[24] Sayarshad HR, Chow JY. Non-myopic relocation of idle mobility-on-demand vehicles as a dynamic location-allocation-queueing problem. Transp Res Part E Logist Transp Rev 2017;106:60–77.

[25] Wen J, Zhao J, Jaillet P. Rebalancing shared mobility-on-demand systems: A reinforcement learning approach. In *2017 IEEE 20th International Conference on Intelligent Transportation Systems (ITSC)*, 2017, October, pp. 220–225.

[26] Ma TY, Rasulkhani S, Chow JY, Klein S. A dynamic ridesharing dispatch and idle vehicle repositioning strategy with integrated transit transfers. Transp Res Part E Logist Transp Rev 2019;128:417–442.

[27] Pouls M, Meyer A, Ahuja N. Idle vehicle repositioning for dynamic ride-sharing. *arXiv preprint arXiv:2008.07957*, 2020.

[28] Melendez, K. A., Das, T. K., & Kwon, C. (2020). Optimal operation of a system of charging hubs and a fleet of shared autonomous electric vehicles. *Applied Energy*, *279*, 115861.

[29] Yi Z, Smart J. A framework for integrated dispatching and charging management of an autonomous electric vehicle ride-hailing fleet. Transp Res D Transp Environ 2021;95:102822.

[30] de Souza F, Gurumurthy KM, Auld J, Kockelman KM. An optimization-based strategy for shared autonomous vehicle fleet repositioning. In *Proceedings of the 6th International Conference on Vehicle Technology and Intelligent Transport Systems*, 2020, May, pp. 370–376.

[31] Dean MD, Gurumurthy KM, de Souza F, Auld J. Synergies between repositioning and charging strategies for shared autonomous electric vehicle (SAEV) fleets. In the 2021 International Symposium on Transportation Data and Modeling, 2021.

[32] Yao H, Wu F, Ke J, Tang X, Jia Y, Lu S, Li Z. Deep multi-view spatial-temporal network for taxi demand prediction. In *Thirty-Second AAAI Conference on Artificial Intelligence*, 2018, April.

[33] Yao, H., Tang, X., Wei, H., Zheng, G., & Li, Z. (2019, July). Revisiting spatial-temporal similarity: A deep learning framework for traffic prediction. In Proceedings of the AAAI Conference on Artificial Intelligence (Vol. 33, pp. 5668-5675).

[34] Lee D, Jung S, Cheon Y, Kim D, You S. Forecasting taxi demands with fully convolutional networks and temporal guided embedding. 2018.

[35] Xu C, Ji J, Liu P. The station-free sharing bike demand forecasting with a deep learning approach and large-scale datasets. Transp Res Part C Emerg Technol 2018;95:47–60.

[36] Chen Z, Zhao B, Wang Y, Duan Z, Zhao X. Multitask learning and GCN-based taxi demand prediction for a traffic road network. Sensors 2020;20:3776.

[37] SEO-Taxi. Taxi operation analysis data on major roads in Seoul, https://data.seoul.go.kr/ [accessed 1 July 2019].

[38] Ronneberger O, Fischer P, Brox T. U-net: Convolutional networks for biomedical image segmentation. In *International Conference on Medical Image Computing and Computer-assisted Intervention*, 2015, October, pp. 234–241, Springer.

[39] Curran-Everett D. Explorations in statistics: The log transformation. Adv Physiol Educ 2018;42:343–347.

[40] Kipf TN, Welling M. Semi-supervised classification with graph convolutional networks. *arXiv preprint arXiv:1609.02907*, 2016.

[41] Dijkstra EW. A note on two problems in connexion with graphs. Numer Math 1959;1:269–271.

[42] Seoul Metropolitan Government. (2019). Seoul road speed statistics. Seoul Metropolitan Government, https://bigdata.seoul.go.kr/; 2019 [accessed 26 August 2019].

[43] Lee U, Kang N, Lee I. Selection of optimal target reliability in RBDO through reliability-based design for market systems (RBDMS) and application to electric vehicle design. Struct Multidiscip Optim 2019;60:949–963.

[44] EV Specifications. 2019 Nissan Leaf SV Plus, https://www.evspecifications.com/en/model/bbbd9a; 2019 [accessed 20 June 2019].

[45] EV Monitor, https://www.ev.or.kr/evmonitor; 2020 [accessed 24 January 2020].

[46] Tansel BC, Francis RL, Lowe TJ. State of the art—location on networks: a survey. Part I: the p-center and p-median problems. Manag Sci 1983;29:482–497.

[47] The Mack Institute. Analysis shows continued industry-wide decline in electric vehicle battery costs. The Mack Institute, https://mackinstitute.wharton.upenn.edu/2018/electric-vehicle-battery-costs-decline/, 2017.

[48] Simpson A. *Cost-benefit analysis of plug-in hybrid electric vehicle technology* (No. NREL/CP-540-40485), National Renewable Energy Lab (NREL), Golden, CO (United States), 2006.

[49] EERE. Study shows average cost of electric vehicle charger installations. U.S. Department of Energy, 2016. https://www.energy.gov/eere/vehicles/fact-910-february-1-2016-study-shows-average-cost-electric-vehicle-charger.